J Mater Sci (2011) 46:2331–2337
DOI 10.1007/s10853-010-5078-z

EPR and photoluminescence properties of combustion-synthesized $ZnAl_2O_4:Cr^{3+}$ phosphors

Vijay Singh · R. P. S. Chakradhar · J. L. Rao · Ho-Young Kwak

Received: 3 September 2010 / Accepted: 10 November 2010 / Published online: 30 November 2010

Abstract An efficient red emitting $ZnAl_2O_4:Cr^{3+}$ powder phosphor material was prepared at furnace temperatures as low as 500 °C by using the combustion method. The prepared powders were analyzed by X-ray diffraction and scanning electron microscopy techniques. The optical properties were studied using photoluminescence technique. The EPR spectra exhibit an intense resonance signal at $g = 3.74$ which is attributed to Cr^{3+}–Cr^{3+} pairs, and the weak resonance signal of at $g = 1.97$ is attributed to Cr^{3+} single ion transition. The spin population (N) has been evaluated as a function of temperature. The excitation spectrum exhibits two broad bands in the visible region which are characteristic of Cr^{3+} ions in octahedral symmetry and the emission spectrum exhibits zero-phonon line frequencies along with vibronic frequencies. The crystal field parameter (Dq) and Racah parameters (B and C) have been evaluated and discussed.

V. Singh (✉) · H.-Y. Kwak (✉)
Department of Mechanical Engineering, Chung-Ang University, Seoul 156-756, Korea
e-mail: vijayjiin2006@yahoo.com

H.-Y. Kwak
e-mail: kwakh@cau.ac.kr

R. P. S. Chakradhar
Glass Technology Laboratory, Central Glass and Ceramic Research Institute (CSIR), Kolkata 700032, India

J. L. Rao
Department of Physics, Sri Venkateswara University, Tirupati 517502, India

Introduction

Metal aluminates with spinel structure are widely used as high-temperature material, catalyst, catalyst support, optical coating for spacecrafts and have applications as the best wide band gap semiconductor material for photoelectric devices [1–3]. Based on these, much more efforts have been devoted to study the luminescent properties of the impurity-doped $ZnAl_2O_4$ [4–6]. In particular, Cr^{3+} ion dopants are currently receiving a great deal of attention due to the rapid development of laser diodes [7–9]. This study deals with the effect of Cr-doping on some of the optical and photoluminescence properties of $ZnAl_2O_4$. This host has the crystal structure of $Zn^{2+}Al_2{}^{3+}O_4$ and the spinel unit cell related to the cubic space group 0_h^7 ($Fd3m$) with eight formula units per cell. In this Zn site has tetrahedral coordination with full T_d site symmetry, while the Al site has sixfold distorted octahedral coordination related to the D_{3d} point group [10–12]. There is some ambiguity on the location of Cr^{3+} when these spinels are doped with Cr. In this connection electron paramagnetic resonance and optical spectra can give information about the manner in which Cr^{3+} ion interacts with the lattice. Though many spectroscopic studies on the $ZnAl_2O_4$-doped with rare earths have been reported in the recent past [13–15], reports on spectroscopy on Cr-doped $ZnAl_2O_4$ are rare.

Precipitation [16], solid-state reaction [17], hydrothermal synthesis [18], sol–gel [19], and combustion synthesis [20] have been used successfully in the preparation of many oxide-based materials, especially in the recent years. Among these methods, combustion synthesis, a relatively newer chemical route, is taking a prominent role as it is a fast and cheap method, which saves energy and time, and avoids the post-calcination necessity. This article reports the use of a viable combustion process for the preparation of Cr^{3+}-doped $ZnAl_2O_4$ phosphor. The prepared combustion product was characterized by X-ray diffraction (XRD), scanning electron microscopy (SEM), photoluminescence (PL), and electron paramagnetic resonance (EPR) techniques. Our studies reveal that chromium is incorporated as Cr^{3+} ions in the prepared $ZnAl_2O_4$.

Experimental

0.01% Cr^{3+} ions-doped $ZnAl_2O_4$ phosphor ($ZnAl_2O_4$:Cr) was prepared by heating zinc/aluminum/chromium nitrates in stoichiometric proportions with fuel (urea) at temperature around 500 °C. Nitrate to urea ratio was calculated as described elsewhere [21, 22]. The synthesis was carried out as follows: first, the nitrates and urea were mixed in an agate mortar to form a paste which was then transferred to a china dish. Afterward, the china dish was placed in a furnace preheated at 500 ± 10 °C. The paste underwent dehydration at lower temperatures and decomposition resulting in deflation with the simultaneous evolution of large amounts of gases. After this step, the foam was automatically ignited, giving a voluminous and fluffy product. This whole process lasted about 5 min. The dish was then taken out of the furnace, and the foamy product was crushed into a fine powder. This powder was used for characterization.

The compound, so prepared, was identified using powder XRD. X-ray diffractogram was recorded (X' pert, Philips, Netherlands) using CuK_α radiation ($\lambda = 0.15418$ nm) in the 2θ range from 10 to 70°. Powder morphology was studied using scanning electron microscope (JSM-5610LV, JEOL, Japan). Room temperature photoluminescence measurements were carried out using an AMINCO-Bowman Series 2 luminescence spectrometer at room temperature and also with a confocal laser micro-Raman spectrometer (Raman, LABRAM-HR) with 488 nm laser excitation. EPR measurements were carried out using a Bruker EMX 10/12 X-band ESR spectrometer.

Results and discussion

X-ray diffraction

X-ray diffraction (XRD) pattern of the as-prepared $ZnAl_2O_4$:Cr is shown in Fig. 1a. All diffraction peaks could be indexed to the single phase of $ZnAl_2O_4$ and matched perfectly with the standard pattern (JCPDS 82-1043; Fig. 1b). The peaks and intensities of the synthesized powder and that of standard were well matched. Mono cubic $ZnAl_2O_4$ spinel is formed in a single step, at the furnace temperature (500 °C), and a further calcination treatment is not necessary. Also, the transformation of the products to this spinel is complete.

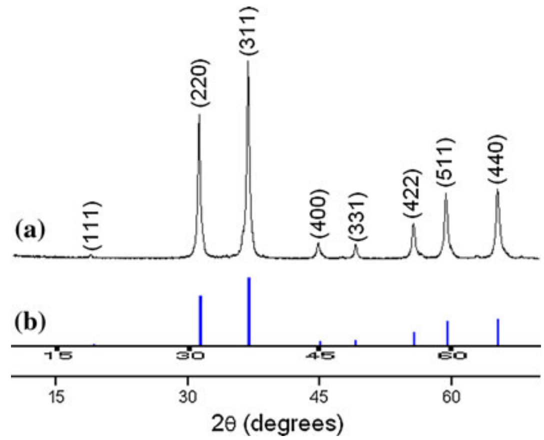

Fig. 1 Powder XRD patterns of (*a*) $ZnAl_2O_4$:Cr and (*b*) $ZnAl_2O_4$ (JCPDS, No. 82-1043)

Scanning electron microscopy

Figure 2 shows the SEM micrographs of $ZnAl_2O_4$:Cr with low and high magnification. Low-resolution SEM micrographs show that the crystallites have no uniform shape. The morphology of the powders consists of faceted crystals with apparent diverse sizes (Fig. 2a). This non-uniformity of shape is due to the non-uniform distribution of temperature and mass flow in the combustion flame. Besides the faceted crystals the powders show number of voids and pores, which result from the escaping gases during combustion. Figure 2b is magnified to get Fig. 2c. From higher magnification it is clear that faceted crystals are composed of very small crystals. All these features are expected from combustion product.

Electron paramagnetic resonance study

Electron paramagnetic resonance spectroscopy is a sensitive technique for studying nature and symmetry of paramagnetic ions. The authors, therefore, carried out EPR studies. Figure 3 shows the EPR spectrum of $ZnAl_2O_4$:Cr^{3+} powder phosphor sample at room temperature. The EPR spectrum exhibits an intense resonance signal centered at $g = 3.74$ and a weak resonance signal at $g = 1.97$. The Cr^{3+} ions (d^3) tend to occupy approximately octahedral sites in several hosts [23], as they are Jahn–Teller distortion inactive. In the absence of magnetic field, d^3 ion splits into ±3/2 and ±1/2 Kramers doublets separated by $2D$, where D is the zero-field splitting parameter. On application of magnetic field the degeneracy is lifted and one can observe three resonances corresponding to $Ms = -3/2 \leftrightarrow -1/2$, $-1/2 \leftrightarrow +1/2$, and $+1/2 \leftrightarrow +3/2$,

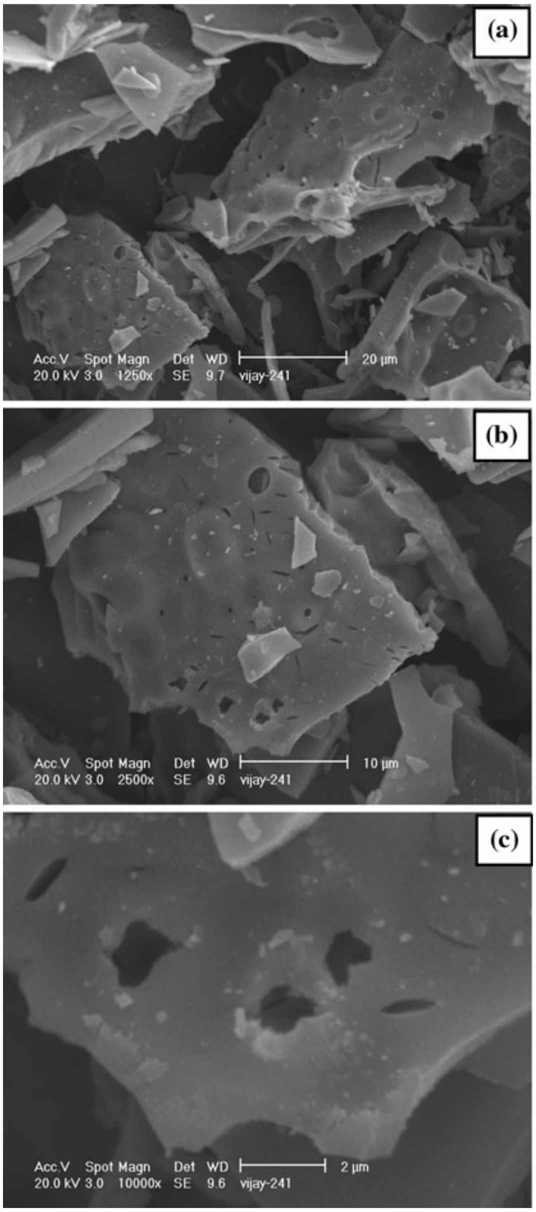

Fig. 2 SEM micrographs of the $ZnAl_2O_4$:Cr at low and high magnification

transitions at $g\beta B - 2D$, $g\beta B$, and $g\beta B + 2D$, respectively. In general the powder samples containing Cr^{3+} are difficult to interpret. If $D = 0$ one can observe only a single resonance line centered around $g = 1.98$. If all the transitions are observed, then the separation between extreme set of lines will be $4D$. On the other hand, if D is very large compared to the microwave frequency, a line occurs at around $g = 4.0$ [24]. Barry [25] also reported that in strong crystal fields, where the zero-field splitting exceeds the energy of microwave, the EPR spectra of Cr^{3+} is dominated by a peak at $g_{eff} = 3.8$ in the case of uniaxial crystal field symmetry.

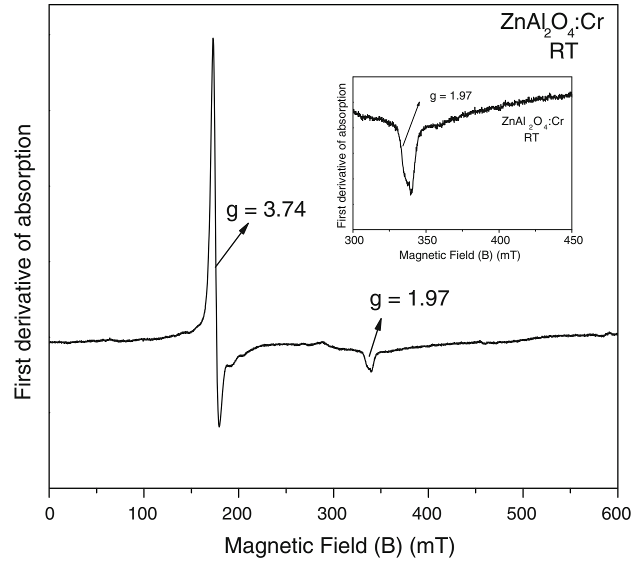

Fig. 3 EPR spectrum of $ZnAl_2O_4$:Cr at room temperature

Recently Giada Lorenzi et al. [26] studied the EPR spectrum of Cr bearing gahnite ($ZnAl_2O_4$) pigment at X and W band frequencies. They also observed two resonance signals corresponding to g values of 3.87 and 2.05, respectively. Moreover, the intensity of the resonance signal at $g = 3.87$ is high when compared to the resonance signal at $g = 2.05$. Similar observations are noticed in this study. The difference in EPR signals and its intensity variation may be attributed to the difference in the Cr^{3+} environment in the host lattice sample. The intense resonance signal is attributed to Cr^{3+} pair transitions, and the weak resonance signal is attributed to Cr^{3+} single ion transition. Similar interpretation was given by Jun Ren Lo et al. [27]. The appearance of intense EPR signal of Cr^{3+} ions in the low magnetic field range indicates that the zero-field splitting (D) is relatively large in comparison with the energy of the microwave radiation used in the X-band spectrometer. The EPR spectrum is also recorded at different temperatures as shown in Fig. 4, in order to find the effect of temperature on resonance signals.

Spin concentration (N)

The spin concentration (N) can be calculated by comparing the area under the absorption curve with that of a standard ($CuSO_4 \cdot 5H_2O$ in this study) of known concentration. Weil et al. [28] gave the following expression which includes the experimental parameters of both sample and standard:

$$N = \frac{A_x(\text{Scan}_x)^2 G_{std}(B_m)_{std}(g_{std})^2[S(S+1)]_{std}(P_{std})^{1/2}}{A_{std}(\text{Scan}_{std})^2 G_x(B_m)_x(g_x)^2[S(S+1)]_x(P_x)^{1/2}}[Std] \quad (1)$$

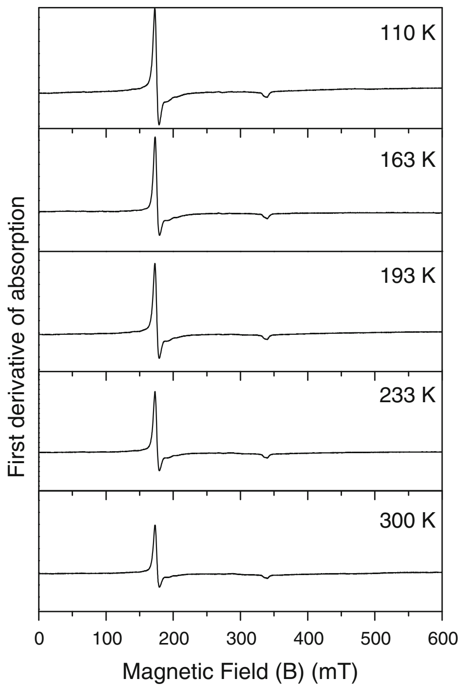

Fig. 4 EPR spectra of $ZnAl_2O_4$:Cr phosphor as a function of temperature

where A is the area under the absorption curve, which can be obtained by double integrating the first-derivative EPR absorption curve, scan is the magnetic field corresponding to a unit length of the chart, G is the gain, B_m is the modulation field width, g is the g factor, and S is the spin of the system in its ground state. P is the power of the microwave source. The subscripts '*x*' and '*std*' represent the corresponding quantities for the $ZnAl_2O_4$:Cr phosphor and the reference ($CuSO_4{\cdot}5H_2O$), respectively. The value of N has been calculated for $g = 3.74$ as a function of temperature. It is observed that as the temperature is lowered, N increases obeying the Boltzmann law. Figure 5 shows a plot of Log N versus $1/T$. The data are least square fit to a straight line Log $N = 56.8\ (1/T) + 20.60$. The activation energy thus calculated is found to be 1.779×10^{-21} J (~0.011 eV) which is the same order expected for paramagnetic ions.

Photoluminescence study

Excitation spectrum

The excitation spectrum for $ZnAl_2O_4$:Cr is shown in Fig. 6a. The spectrum exhibits two broad absorption bands at 535 nm (~18685 cm^{-1}) and 421 nm (~23750 cm^{-1}). In addition to this a weak band at 475 nm (~21050 cm^{-1}) and a small hump at about 400 nm (~25000 cm^{-1}) are also observed. The intensity and position of these bands suggest that Cr^{3+} ions are in octahedral symmetry. The optical absorption spectrum of Cr^{3+} ions in Oh symmetry has been characterized extensively [29]. One observes two intense broad bands corresponding to $^4A_{2g} \rightarrow {}^4T_{2g}$, $^4T_{1g}$ spin-allowed transitions. The separation between them being typically 6000–7500 cm^{-1}. Additional weak and narrow bands associated to the ^2E_g, $^2T_{1g}$, and $^2T_{2g}$ excited states are also expected. Furthermore, luminescence emission is usually observed. The broad band at 535 nm (~18685 cm^{-1}) is assigned to $^4A_{2g}$ (F) $\rightarrow$ $^4T_{2g}$ (F) transition (ν_1). The other broad band and 421 nm and the small hump at ~400 nm (~25000 cm^{-1}) are assigned to $^4A_{2g}$ (F) $\rightarrow$ $^4T_{1g}$ (F) transition (ν_2). The weak band observed at ~475 nm (~21050 cm^{-1}) is assigned to $^4A_{2g}$ (F) $\rightarrow$ $^2T_{2g}$ (G) transition.

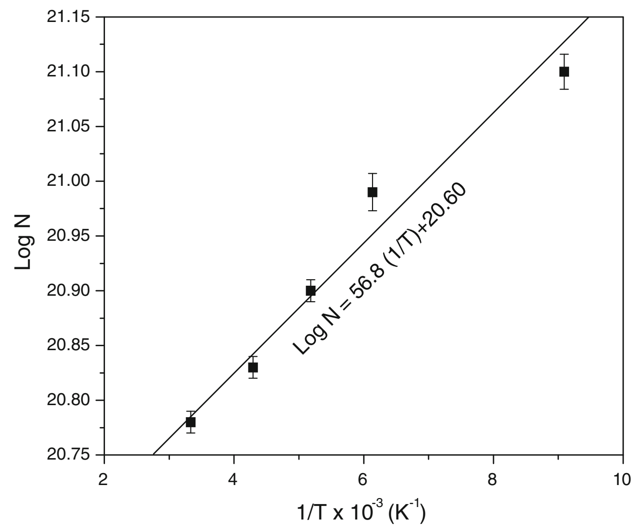

Fig. 5 A plot of logarithmic intensity (log N) versus $1/T$ at different temperatures

The (ν_1) band gives the crystal field splitting parameter, 10 Dq. The Racah parameter B was calculated by assigning a mean value for the (ν_2) bands by the using the relation [30]:

$$B = \frac{(2\nu_1^2 + \nu_2^2 - 3\nu_1\nu_2)}{15\nu_2 - 27\nu_1}\ldots \quad (2)$$

The calculated crystal field (Dq) and Racah parameter (B) in cm^{-1} along with those reported for similar Cr^{3+} ions in spinels [10, 26, 31] are presented in Table. 1. The value of inter-electronic repulsion parameter B_{free} for Cr^{3+} ion is 918 cm^{-1} [32]. A comparison with this study indicates that B is decreased by 42% from the free ion value. This decrease is caused by bond covalency. In the Tanabe-Sugano diagram [33] the crossing of the ^2E and $^4T_2$ levels occurs near $Dq/B = 2.3$. Values higher than 2.3 correspond to strong crystal field. The value of Dq/B obtained in this study ($Dq/B = 3.49$) indicates that Cr^{3+} ions are situated in strong crystal field where the ^2E is the lowest. Accordingly

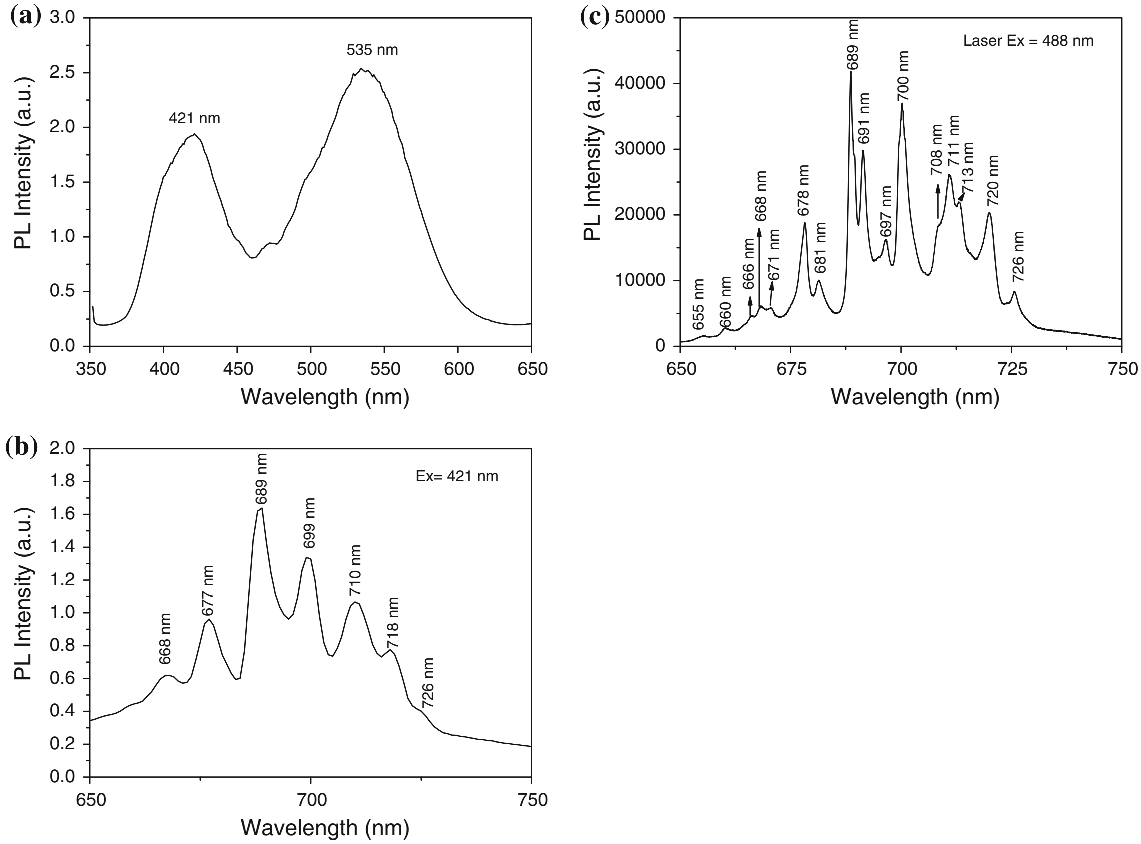

Fig. 6 Typical photoluminescence spectrum of Cr^{3+}-doped $ZnAl_2O_4$: **a** excitation spectrum of $ZnAl_2O_4$:Cr ($\lambda_{em} = 689$ nm), **b** emission spectrum of $ZnAl_2O_4$:Cr ($\lambda_{ex} = 421$ nm), and **c** emission spectrum of $ZnAl_2O_4$:Cr (Laser $\lambda_{ex} = 488$ nm)

Table 1 Comparison of crystal field (*Dq*) and Racah (*B*) parameter reported in the literature for Cr^{3+} ions in spinels

Crystal field parameter (*Dq*)	$MgAl_2O_4$ [10]	$BaAl_2O_4$ [31]	$ZnAl_2O_4$ [26]	Preset study
10 *Dq*	18250	18110	18800	18685
B (in cm^{-1})	700	533	550	534

this phosphor should be a photoluminescence associated with a spin and parity forbidden $^2E \rightarrow {}^4A_2$ transition.

Emission spectrum

The emission spectrum of $ZnAl_2O_4$:Cr upon excitation with 421 nm and the emission spectrum with laser excitation of 488 nm are shown in Fig. 6b, c, respectively. In Fig. 6b a few lines are observed whereas in Fig. 6c a number of peaks are observed. The authors analyzed the emission lines observed in Fig. 6c only. The room temperature emission spectrum consisting of a prominent line at 689 nm and another line at 691 nm. These are attributed to R_2 and R_1 components of the crystal field *R* line.

$ZnAl_2O_4$ (normal spinel) belong to the O_h^7 group with a tetrahedral coordination for the Zn^{2+} ion at 8a positions and a trigonal distorted octahedron (D_{3d} symmetry) surrounding the Al^{3+} site at 16*d* positions. Octahedrally Cr^{3+} ions doping the trigonally distorted CrO_6 octahedron is surrounded by six Al^{3+} ions and by six Zn^{2+} ions. In normal spinels all the octahedral positions are occupied by Al^{3+} ions while all the tetrahedral positions are occupied by Zn^{2+} ions. If the spinel is partially inverse, some Zn^{2+} ions occupy 16*d* positions and some Al^{3+} ions occupy 8*a* positions [34].

Some spinels ($MgAl_2O_4$) undergo inversion to some extent when heated between 750 and 900 °C without annealing [35].The inversion must occur to a considerable degree in our phosphor as evident from the appearance of additional lines in the spectrum due to $^2E \rightarrow {}^4A_2$ emissions, which are the result of changes in the position of Cr^{3+} energy levels in the inverted versus normal sites.

The sharp and intense emission lines have been observed for Cr^{3+} ions and are identified by previous reports [36, 37]. They are so-called R and N lines of the $^2E \rightarrow {}^4A_2$ transition of Cr^{3+} ions associated with vibronic site bands. The *R* lines belong to regular 16*d* site of the spinel structure whereas the N lines have been attributed to the Cr^{3+} ions perturbed by inversion between Zn^{2+} and Al^{3+} within the first two coordination spheres [38].

Table 2 Observed band positions in the emission spectrum of $ZnAl_2O_4$:Cr phosphor upon laser excitation wavelength of 488 nm

System	Line	Wavelength (nm)	Wavenumber (cm^{-1})
$ZnCrAl_2O_4$:Cr	R_2	689	14510 (Zero-phonon line)
	R_1	691	14468
		697	14343
	N_1	700	14282
	N_2	708	14120
	N_3	711	14061
	N_4	713	14021
		720	13885
		726	13770

Therefore, the observed lines at 689 and 691 nm are R lines of Cr^{3+} ions in octahedral sites. The experimentally observed band positions and their vibrational energies are listed in Table. 2. The R lines originate from transition $^2E \rightarrow {}^4A_2$ of Cr^{3+} ions substituting at the 16*d* (D_{3d}). According to Boltzmann law, the intensity of the higher energy line (R_2) should be lower than the intensity of the lower energy line (R_1). But the reverse trend is observed in this study. It can be confirmed only if one can measure the temperature dependence of luminescence studies. The origin of weaker lines, called *N* lines (N_1, N_2, N_3, N_4), is ascribed to closely coupled pairs of Cr^{3+} ions. The formation of Cr^{3+}–Cr^{3+} pairs is also confirmed by the presence of intense resonance signal at $g = 3.74$. The N lines can be interpreted as zero-phonon lines of different luminescence centers and are, therefore, spectroscopic analogs of the R line.

Conclusions

It is possible to obtain Cr-doped $ZnAl_2O_4$ red emitting phosphors using a combustion synthesis method. Urea nitrates are not only inexpensive but also readily available and have a great potential for large-scale application in combustion synthesis of aluminate-based powder phosphors. Moreover, combustion requires lower processing temperatures short time to synthesize the phosphor. Luminescence studies exhibited characteristic features of Cr^{3+} ions, and EPR spectra also revealed signals due to Cr^{3+} ions in $ZnAl_2O_4$ phosphor material. The EPR spectrum exhibits two resonance signals centered at $g = 3.74$ and $g = 1.97$ which are attributed to Cr^{3+}–Cr^{3+} pairs and Cr^{3+} single ion transition, respectively. The appearance of intense EPR signal in the low magnetic field range indicates that the zero-field splitting is very large. It is observed that the number of spins participating in resonance increases with decreasing temperature obeying Boltzmann law. The excitation spectrum consists of two broad absorption band characteristics of Cr^{3+} ions in octahedral symmetry. The *Dq*/*B* value indicates the strong crystal field environment present in the phosphor. The emission spectrum consists of a number of lines like zero-phonon lines (R lines), N lines, as well as phonon side bands.

Acknowledgements Dr. Vijay Singh expresses his thanks to the Chung-Ang University, Seoul (South Korea) for providing the Research Assistant Professorship. Dr. RPSC thanks Dr. H. S. Maiti, Director, CGCRI, and Dr. Ranjan Sen, Head, GTL lab, CGCRI for their constant encouragement.

References

1. Cordoro JF, Houghton MI, Long LE, Manhattan Beach CA (1998) US Patent No. 5,807,909
2. Sampath SK, Kandive DG (1999) J Phys Condens Mater 11:3635
3. Cordoro JF (2000) US Patent No. 6,099,637, 8 Aug 2000
4. Yoo S, Paek U-C, Han W-T (2002) J Non-Cryst Solids 303:291
5. Duan X, Yuan D, Sun Z, Luan C, Pan D, Dong X, Lv M (2005) J Alloys Compd 386:311
6. Botao W, Qiu J, Peng M, Ren J, Jiang X, Zhu C (2007) Mater Res Bull 42:762
7. Solntsev VP, Pestryakov EV, Alimpiev AI, Tsvetkov EG, Matrosov VN, Trunov VI, Petrov VV (2003) Opt Mater 24:519
8. Jiang B, Zhao Z, Xiaodong X, Song P, Wang X, Jun X, Deng P (2007) Opt Mater 29:1188
9. Yagi H, Yanagitani T, Yoshida H, Nakatsuka M, Ueda K (2007) Opt Laser Technol 39:1295
10. Wood DL, Imbusch GF, Macfarlane RM, Kisliuk P, Larkin DM (1968) J Chem Phys 48:5255
11. Wells AF (1978) Structural inorganic chemistry, 5th edn. Clarendon Press, Oxford, p 594
12. O'Neill H, Dollase W (1994) Phys Chem Miner 20:541
13. Lou Z, Hao J (2004) Thin Solid Films 450:334
14. Wang SF, Feng G, Lu MK, Cheng XF, Zou WG, Zhou GJ, Wang SM, Zhou YY (2005) J Alloys Compd 394:255
15. Barros BS, Melo PS, Kiminami RHGA, Costa ACFM, de Sá GF, Alves S Jr (2006) J Mater Sci 41:4744. doi:10.1007/s10853-006-0035-6
16. Popovici E-J, Muresan L, Amalia H, Indrea E, Vasilescu M (2007) J Alloys Compd 434-435:809
17. Arean CO, Sintes BS, Palomino GT, Carbonell CM, Scalona Platero E, Parra Soto JB (1997) Microporous Mater 8:187
18. Chen Z, Shi E, Zheng Y, Li W, Wu N, Zhong W (2002) Mater Lett 56:601
19. Mathur S, Veith M, Haas M, Haoshen, Lecerj N, Huch V (2001) J Am Ceram Soc 84:1921
20. Ekambarama S, Iikubo Y, Kudo A (2007) J Alloys Compd 433:237
21. Kingsley JJ, Patil KC (1988) Mater Lett 6:427
22. Arul Dhas N, Patil KC (1993) J Solid State Chem 102:440
23. Orgel LE (1966) An introduction to transition metal chemistry. Metheun, London
24. Misra SK, Isber S, Chand P (2000) Phys B 105:291
25. Barry TI (1969) J Mater Sci 4:485. doi:10.1007/BF00550209
26. Lorenzi G, Baldi G, Benedetto FD, Faso V, Pardi LA, Romanelli M (2006) J Eur Ceram Soc 26:125
27. Jun-Ren L, Ezhilvalavan S, Tseng T-Y (1999) Jpn J Appl Phys 38:1390

28. Weil JA, Bolton JR, Wertz JE (1994) Electron paramagnetic resonance-elementary theory and practical applications. Wiley, New York, p 498
29. Henderson B, Imbush GF (1989) Optical spectroscopy of inorganic solids. Clarendon Press, Oxford
30. Perumareddy JR (1969) Coord Chem Rev 4:73
31. Vijay Singh RPS, Chakradhar JL, Rao J-JZ (2008) Mater Chem Phys 111:143
32. Orton JW (1968) An introduction to transition group ions in crystals. ILIFFE Book Ltd, London
33. Tanabe Y, Sugano S (1954) J Phys Soc Jpn 9:753
34. Nie W, Michael-Calendini FM, Linares C, Boulon G, Daul C (1990) J Lumin 46:177
35. Derkosh J, Mihendra W, Preisinger A (1976) Spectrochim Acta 32A:1759
36. Boulon G (1987) Mater Chem Phys 16:301
37. Derkosch J, Mikenda W, Pressinger A (1977) J Solid State Chem 22:127
38. Mikenda W, Preisinger A (1981) J Lumin 26:67